

IN-27
20313

NASA
Technical Memorandum 105565

Army Research Laboratory
Memorandum Report ARL-MR-15

28P

Fracture Behavior of Ceramics Under Displacement Controlled Loading

Anthony Calomino
*National Aeronautics and Space Administration
Lewis Research Center
Cleveland, Ohio*

David Brewer
*Vehicle Propulsion Directorate
U.S. Army Research Laboratory
Lewis Research Center
Cleveland, Ohio*

Louis Ghosn
*Sverdrup Technology, Inc.
Lewis Research Center Group
Brook Park, Ohio*

July 1994

N95-11248
Unclas
G3/27 0020313
(NASA-TM-105565) FRACTURE BEHAVIOR OF CERAMICS UNDER DISPLACEMENT CONTROLLED LOADING (NASA, Lewis Research Center) 26 p



National Aeronautics and Space Administration



Trade names or manufacturers' names are used in this report for identification only. This usage does not constitute an official endorsement, either expressed or implied, by the National Aeronautics and Space Administration.

Fracture Behavior of Ceramics under
Displacement Controlled Loading

By

Anthony Calomino¹, David Brewer², Louis Ghosn³

Summary

A Mode I fracture specimen and loading method has been developed which permits the observation of stable, subcritical crack extension in monolithic and toughened ceramics. The developed technique was used to conduct room temperature tests on commercial grade alumina (Coors' AD-995) and silicon nitride (Norton NC-132). The results of these tests are reported. Crack growth for the alumina remained subcritical throughout testing revealing possible effects of environmental stress corrosion. The crack growth resistance curve for the alumina is presented. The silicon nitride tests displayed a series of stable (slow) crack growth segments interrupted by dynamic (rapid) crack extension. Crack initiation and arrest stress intensity factors, K_{IC} and K_{Ia} , for silicon nitride are reported. The evolution of the specimen design through testing is briefly discussed.

¹NASA LeRC

²U.S. Army, AVSCOM

³Sverdrup Technologies Inc.

Introduction

The ability to directly observe, measure and rigorously analyze subcritical growth behavior in polycrystalline materials is imperative for accurate assessment of a material's fracture response and structural reliability. It is generally accepted that time-dependent failure of ceramics results from the subcritical growth of cracks from preexisting flaws¹⁻⁴. Such subcritical growth, or possibly realignment of inherent material flaws, can severely affect the critical conditions for failure and the structural integrity of a ceramic component. Since subcritical growth would occur at loading levels below Fast-Fracture predictions, failure analyses could be non-conservative. It is obvious, then, that accurate observation of subcritical crack growth behavior is extremely important to model development and predictive analyses. Unfortunately, much of the information obtained for subcritical crack growth in ceramics has been provided by several non-standardized test procedures⁵⁻¹⁰. The uncertainties associated with load history, applied stresses, and crack tip geometries for these test procedures cloud a clear evaluation of a material's fracture response.

An effective approach to generating stable crack extension would involve fixed displacement loading at the crack mouth. Under fixed displacement conditions, most conventional fracture specimens are inherently stable. The stability results from a decrease in the stress intensity factor with increased crack extension under fixed

crack-mouth opening. True fixed displacement loading rarely, if ever, occurs because of specimen/load frame interactions. Specimen compliance increases as crack extension occurs. Elastic energy stored in the loading system is supplied to the specimen during this process. When this stored energy is released it often creates unstable crack growth in extremely stiff and brittle materials, even though the displacement applied by the load frame controller is constant. The Stable Poisson Loaded (SPL) specimen¹¹ developed at NASA Lewis Research Center (LeRC) has been used successfully to quantitatively investigate the subcritical fracture response of monolithic Al_2O_3 and Si_3N_4 ceramics. Initial investigations indicate that stable crack propagation can be controlled over the entire specimen length with this technique.

The objective of this paper is to present an experimental technique, and the related stress results and instrumentation, which can be used to quantitatively investigate subcritical crack growth in brittle materials with high elastic moduli, and report some experimental results generated during the developmental course of these studies.

Procedures, Specimen Development and Material

The ability to establish and observe slow, stable crack growth in monolithic ceramics has been the subject of research at NASA LeRC for approximately three years. The result has been the development of a loading method which minimizes the amount of energy available

for dynamic crack extension. This was accomplished by removing the specimen from direct load linkage, as shown in Fig. 1. Very small displacements are applied to the specimen by the Poisson expansion of a cylinder under compression.

Two specimen designs, the SPL and Modified SPL specimens, have been developed concurrently for use with this loading method. The unknown interfacial fixity (friction effects) between the cylinder, or pin, and the specimen has made computational analyses difficult. A stress analysis of the SPL specimen geometry indicated that removal of material around the pin, Fig. 2, would significantly minimize fixity influence without sacrificing fracture stability. A modified SPL specimen geometry was designed to minimize the unwanted constraint loading while retaining most of the contact stiffness necessary to insure stable crack propagation. The effect that contact friction between the pin and the specimen has on the stress intensity factor, for both the SPL and Modified SPL geometry, can be seen in Fig. 3 and 4. Since totally fixed or free conditions at the specimen-pin interface are unreasonable assumptions, the friction solution, with $\mu=0.4$, was selected as the best stress solution for each specimen geometry. The stress solution for the modified specimen geometry indicates minimal influence from interfacial fixity assumptions. The specifics of the stress analyses will be presented in a future paper¹².

Material and Specimen Preparation

Two types of monolithic, hot pressed ceramic materials were tested, Norton NC-132 silicon nitride, Si_3N_4 , and Coors' AD-995 aluminum oxide, Al_2O_3 . Both materials are commercially available and have an extensive history of experimental testing. Specific material properties, obtained from the manufacturers can be found in Table 1.

Specimens were machined to both the original and modified SPL geometries. All specimens were machined from bulk material such that the direction of crack propagation would be perpendicular to the direction of hot pressing. The load pin contact area was machined with a diamond coring bit and surfaced with diamond grinding mandrel. Significant attention was devoted to establishing the perpendicularity and cylindricity of the hole. A small chevron notch was cut in the specimen with a diamond waffering saw to initiate a straight crack. Specimens were polished to a microstructural finish. This level of finish was necessary to accurately track the crack propagation optically. A succession of diamond slurry abrasive was used with a free abrasive lapping type machine to polish the specimens.

Test Procedures

Displacement controlled testing was achieved by loading a hardened steel pin in compression. Load pins were sized for each test case because of machining tolerances for the pin hole. The proper sized load pin was selected from a set of pins, each diamond ground to

step size increments of 2.5 micrometers. The maximum allowable axial pin stress was 110 MPa, which produced an available maximum displacement of 8.0 micrometers. Since this maximum displacement was not sufficient to propagate a crack, slightly oversize pins were chosen to apply an important 5.0 micrometer initial offset displacement prior to testing.

The loading pins were pressed into the specimens manually with the aide of a simple alignment jig and press. Crack mouth opening displacement (CMOD) was monitored with an extensometer during the pin installation to obtain an accurate opening offset prior to testing. Measurement of this opening offset was necessary for stress intensity computations, which use the total CMOD.

All tests were conducted at room temperature in an ambient environment. Testing was accomplished by monotonically loading the pins in compression. Loading was increased at a constant rate regardless of the observed rate of crack extension. CMOD measurements were made with a small commercial extensometer with a gage length of 6.35 millimeters. Axial pin load and CMOD measurements were recorded on an X-Y plotter, as well as on an analog FM tape recorder. An instrumented SPL specimen is shown in Fig. 5. Crack lengths were optically measured during the test with a traveling microscope, Fig. 6. Optical data was recorded on VHS format video tape for later analysis.

Data recorded on analog tape was digitized during playback after the tests. The rate of digitization varied from 2Hz to 40Hz. Digitization was conducted on a laboratory PC and data files stored magnetically. The digital data was correlated with optical crack length measurements from voice records. Representative experimental applied pin load and CMOD measurements versus crack length are shown in Fig. 7.

Results, Computations and Observations

Typical fracture properties, computed from the stress analysis of the original SPL specimen, are shown in Fig. 8 for both the Coors' AD-995 Al_2O_3 and Norton NC-132 Si_3N_4 materials. Crack growth in the Al_2O_3 material remained subcritical throughout the test. Since a transitional change in crack velocity was not observed for the Al_2O_3 material, K_{Ic} values could not be computed. However, computed fracture toughness values were observed to decrease with crack extension. It was noted that such a result was contrary to a large body of experimental evidence which revealed a fracture toughness which increased during crack extension. These experimental results prompted a re-evaluation of the experimental technique and stress analysis.

It was decided that an investigation of the test specimen and stress model could be accomplished by employing a well tested material which was not known to have serious stress corrosion effects. For this reason, test samples of Norton NC-132 Si_3N_4

material were machined and tested. The results of this test are also displayed in Fig. 8. Similar to the Al_2O_3 tests, computed stress intensity factors for the Si_3N_4 material displayed a decreasing trend with increased crack extension.

One interesting difference noted with the Si_3N_4 material compared to the Al_2O_3 material was a discontinuity in crack propagation rates. As the applied load was increased, subcritical crack extension was observed to occur at an increasing rate. The crack propagation rate increased gradually up to a point of instability. An abrupt change in the propagation rate was observed which resulted in a 'jump' in crack extension. Crack extension was then arrested within the specimen due to the decreasing stress intensity field of the specimen. The unstable portions of crack advance are shown in Fig. 8 as dashed lines. The sequence of subcritical extension leading into unstable propagation was repeated several times in one specimen. The average amount of subcritical extension was 0.5 mm and the average amount of unstable extension was approximately 2 to 3 millimeters for each fracture event.

Both the AD-995 and NC-132 materials again were tested using the modified specimen geometry. The fracture properties computed from these tests are shown in Fig. 9. It was observed that the removal of the constraining material surrounding the load pin did not detrimentally affect specimen stability. Computed properties from the modified specimen were significantly affected at short crack

lengths where the constraint effect was greatest. Computed fracture properties at longer crack lengths indicated little or no change in magnitude.

Once again, subcritical crack extension occurred throughout the test with the Al_2O_3 material where the crack was extended from a depth of 10.55 to 24.5 millimeters. The computed fracture resistance curve for the Al_2O_3 material increased slightly throughout the test. Dynamic crack extension was not observed, thus a value for K_{IC} could not be computed. However, R-curve type K_{Ir} values were observed to increase from 4.2 $\text{MPa}\sqrt{\text{m}}$ at a crack length of 10.5 mm to 4.8 $\text{MPa}\sqrt{\text{m}}$ at a crack length of 24.5 mm.

Tests conducted with the modified test specimen on the Norton material exhibited a behavior similar to the original SPL specimen. The subcritical crack growth rate was observed to accelerate with increased pin load up to instability, as before. The length of subcritical extension averaged approximately 0.5 millimeter and unstable 'jumps' in crack growth were an average of 2 millimeters. Critical stress intensity factors increased from a low of 3.8 $\text{MPa}\sqrt{\text{m}}$ to 4.6 $\text{MPa}\sqrt{\text{m}}$ with the crack achieving a length 28 millimeters at the final arrest. Computed values for K_{IC} and K_{Ia} are given in Table 2 together with the length of the unstable jump preceding each crack arrest.

Discussion of Results

Considering the susceptibility of Al_2O_3 to stress corrosion cracking and the relatively slow rate of loading, continuous subcritical growth was not surprising. However, the material displayed a disturbing trend of decreasing fracture resistance with increasing crack growth when tested in the original SPL geometry. It was noted that such a result was in direct contrast with a large body of experimental evidence indicating an increasing or, at best, flat resistance curve for the Al_2O_3 material.

The decreasing trend for the original SPL specimen data could be related to stress corrosion cracking. However, other experimental behavior did not support such a strong effect from stress corrosion. Crack velocities in the alumina increased shortly after initiation. A reduction in crack velocity was not observed until crack lengths reached approximately 21 mm. Increased crack velocities reduce the reaction time available for stress corrosion and one would expect to measure an increase in the fracture resistance. In direct contrast, fracture resistance measurements decreased with increasing crack velocity. It was suspected therefore that the influence of the pin-specimen friction was not well understood or modeled. It is interesting to note that the fracture resistance curve flattened considerably at a crack length greater than 21 millimeters when crack velocities were noted to decrease.

The decrease in critical fracture properties for a material known

to show no stress corrosion behavior supported the idea that the effects of pin loading were not clearly understood or properly modeled. The stress analyses had revealed that the degree of fixity between the load pin and the specimen would affect the computation of fracture properties. Pin contact friction would be greatest at shorter crack lengths when specimen compliance is lowest. Examination of the stress analysis suggested that the higher frictional forces at shorter crack lengths could artificially produce high fracture toughness.

A negative change in fracture properties was consistent with the argument of relatively high constraint at short crack lengths and lower constraint at longer crack lengths. Frictional forces were greatest where pin constraint was greatest. Referring to Fig. 2, large constraints are generated in regions where the horizontal component of the pin's radial expansion is greater than the vertical or opening component. It was argued, and verified from a stress analysis, that the removal of material around the pin would minimize interfacial friction effects. The disadvantages of removing this material were increased localized deformations, or stored elastic energy, which would adversely affect fracture stability. Due to the unpredictable nature of the interface between the pin and specimen, experimental verification of crack propagation stability was needed.

From the stress analysis results shown in Fig. 4, modification of

the SPL specimen produced the most profound effects at shorter crack lengths, when compared to the stress analysis of the initial geometry shown in Fig. 3. The modified specimen geometry was tested to investigate the specimen stability assumptions and interfacial friction effects. It is interesting to note that although the modification of the specimen did not appreciably change the observed material behavior, the change in trends of computed fracture toughness with crack length changed considerably (see Figures 8 and 9). This observation strengthens the stability assumptions of the loading method and highlights the need to accurately model the influence of constraining forces at the loading pin.

Increasing trends in the fracture toughness of the alumina tested in the modified geometry could be the result of grain interlocking forces along the crack surface, or a reduced activation time for stress corrosion due to increased crack velocity. The computed values for the fracture strength were slightly greater than values reported in literature¹³.

The overall scatter in the computed values for K_{Ic} for the silicon nitride, tested in the modified geometry, was within ten percent of the average value. A slight increasing trend could also conceivably be inferred. Here too crack bridging may affect measured K_{Ic} values, however, each unstable extension of the crack likely destroys some, or possibly all, of the bridging developed by the

previous increment of subcritical growth. Thus each increment of subcritical extension should experience crack surface boundary conditions similar to that of the previous increment. Considering that the variation in K_{Ic} was approximately equal to that reported in literature^{14,15}, it is possible that the trend is not statistically significant.

CONCLUSIONS

- (1) A fracture specimen with supporting stress analysis and testing procedure has been developed to quantitatively investigate the fracture response of brittle non-metallic systems. The test procedure provides for the initiation and controlled extension of a sharp through-thickness crack under pure Mode I loading.

- (2) Frictional forces at the load fixture to specimen interface significantly affected the computed fracture properties of both the Al_2O_3 and Si_3N_4 in the original SPL specimen. The contact problems were minimized by modifying the specimen geometry near the pin hole.

- (3) Crack propagation speeds did not become dynamic for the Al_2O_3 material, but remained subcritical throughout the test. It is anticipated that stress corrosion largely influenced fracture properties.

- (4) Crack propagation in the hot-pressed Si_3N_4 occurred as a series of unstable jumps and crack arrests. Each unstable extension of the crack was preceded by a small increment of subcritical crack growth where crack propagation velocities increased with monotonically applied load.

- (5) Further studies will be undertaken with both materials to determine if the loading rate affects both the fracture toughness and overall material behavior.

Table 1
Physical Properties

Material	E Gpa	Poisson's Ratio	Grain Size Microns Avg.
Coor's AD-995	370	0.20	≤2.2
Norton NC-132	320	0.28	≤3.0

Table 2
Fracture Properties
NC-132

Event (Fig. 9)	K_{Ic} MPa√m	K_{Ia} MPa√m	Δa mm
1.	3.92	3.65	4.7
2.	3.96	3.92	2.4
3.	4.19	4.05	2.8
4.	4.38	4.22	2.6
5.	4.52	4.29	1.9

REFERENCES

- (1) Weiderhorn, S.M., "Subcritical Crack Growth in Ceramics"; 613-46 in *Fracture Mechanics of Ceramics*, Vol. 2, Edited by R.C. Bradt, D.P.H. Hasselman, and F.F. Lange, Plenum Press, New York, 1974
- (2) Jakus, K., Coyne, D.C, and Ritter, J.E., "Analysis of Fatigue Data for Life Time Prediction for Ceramic Materials," *J. Am. Ceram. Soc.*, **13**, 2071-80, 1978
- (3) Singh, D. and Shetty D.K., "Subcritical Crack Growth in Soda Lime Glass in Combined Mode I and Mode II Loading," *J. Am. Ceram. Soc.*, **73** [12] 3597-606 (1990)
- (4) Annis, C.G., Cargill, "Modified Double Torsion Method for Measuring Crack Velocity in NC-132 (Si_3N_4)," 737-744 in *Fracture Mechanics of Ceramics*, Vol. 4, Edited by R.C. Bradt, D.P.H. Hasselman, and F.F. Lange, Plenum Press, New York, 1974
- (5) Bubsey, R.T, Munz D., Pierce, W.S., and Shannon Jr., J.L., "Compliance Calibration of the Short Rod Chevron Notch Specimen for Fracture Toughness Testing of Brittle Ceramics," *Int. J. Fract.*, **18** [11], 153 (1982)
- (6) Nose T., and Fujii T., "Evaluation of Fracture Toughness for Ceramic Materials by a Single-Edge-Pre-cracked-Beam Method,": *J. Am. Ceram. Soc.*, **71** [5] 328 (1988)
- (7) Petrovic, J.J. and Mendiratta, M.G., "Fracture from Controlled Surface Flaws," *Fracture Mechanics Applied to Brittle Materials*, ASTM STP 678. S.W. Freiman, Ed., American Society for Testing Materials, 83-102, 1979
- (8) Ritter, J. E., "Engineering Design and Fatigue Failure of Brittle Materials," pp. 667-86 in *Fracture Mechanics of Ceramics*, Vol. 4, Edited by R.C. Bradt, D.P.H. Hasselman, and F. Lange, Plenum Press, New York, 1978
- (9) Seshadri, S.G., Srinivasan, M., and Weber, G.W., "Evaluation of Slow Crack Growth Parameters for Silicon Carbide Ceramics," *J. Matl. Sci.*, **17**, 1297-1302 (1982)
- (10) Mai, Y.W., and Lawn, B.R., "Crack-Interface Bridging as a Fracture Resistance Mechanism in Ceramics II: Theoretical Fracture Mechanics Model," *J. Am. Ceram. Soc.*, **70** [4] 289-94 (1987)
- (11) Calomino, A.M., and Brewer, D.N., "Controlled Crack Growth Specimen for Brittle Systems," *J. Am. Ceram. Soc.*, **75** [1]

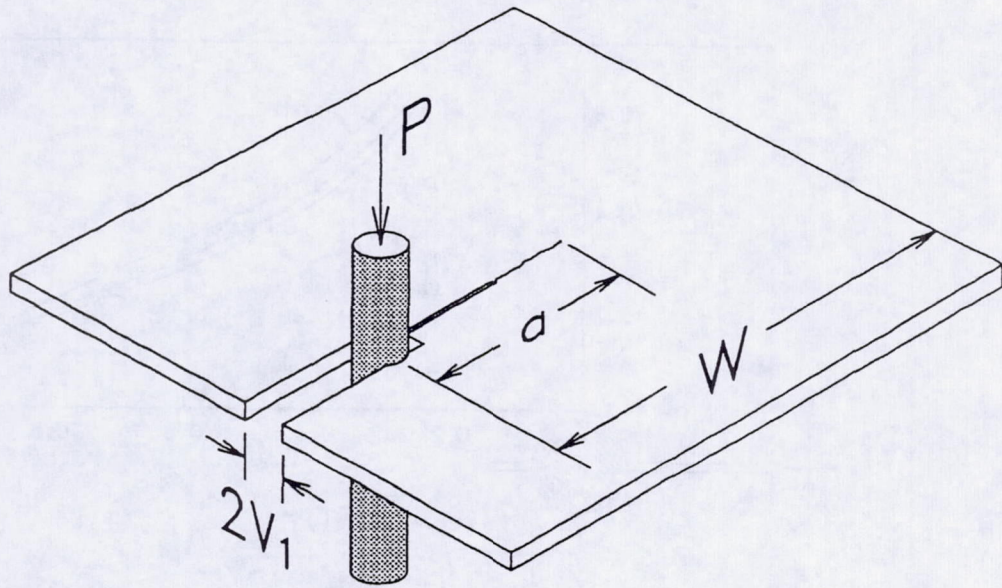


Fig. (1) Modified SPL specimen geometry with the compressed pin loading concept for stable crack growth experiments.

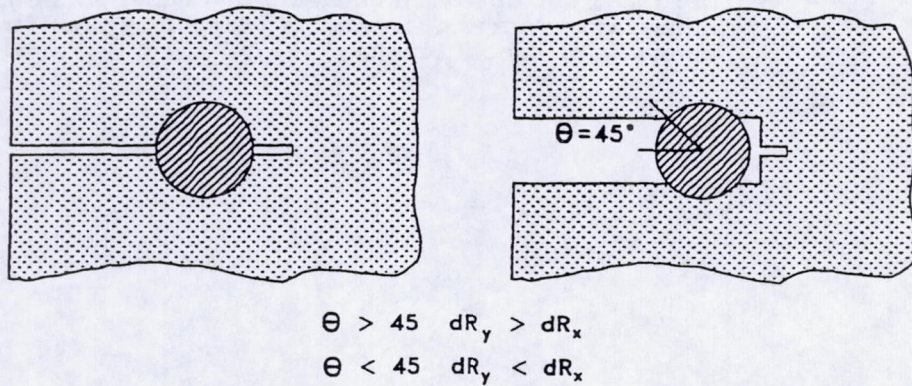


Fig. (2) Pin constraint effects for the initial (a) and modified (b) SPL Specimen Geometry. Removed section for modified geometry occurs where specimen compliance greatly constrains pin expansion, dR_y and dR_x .

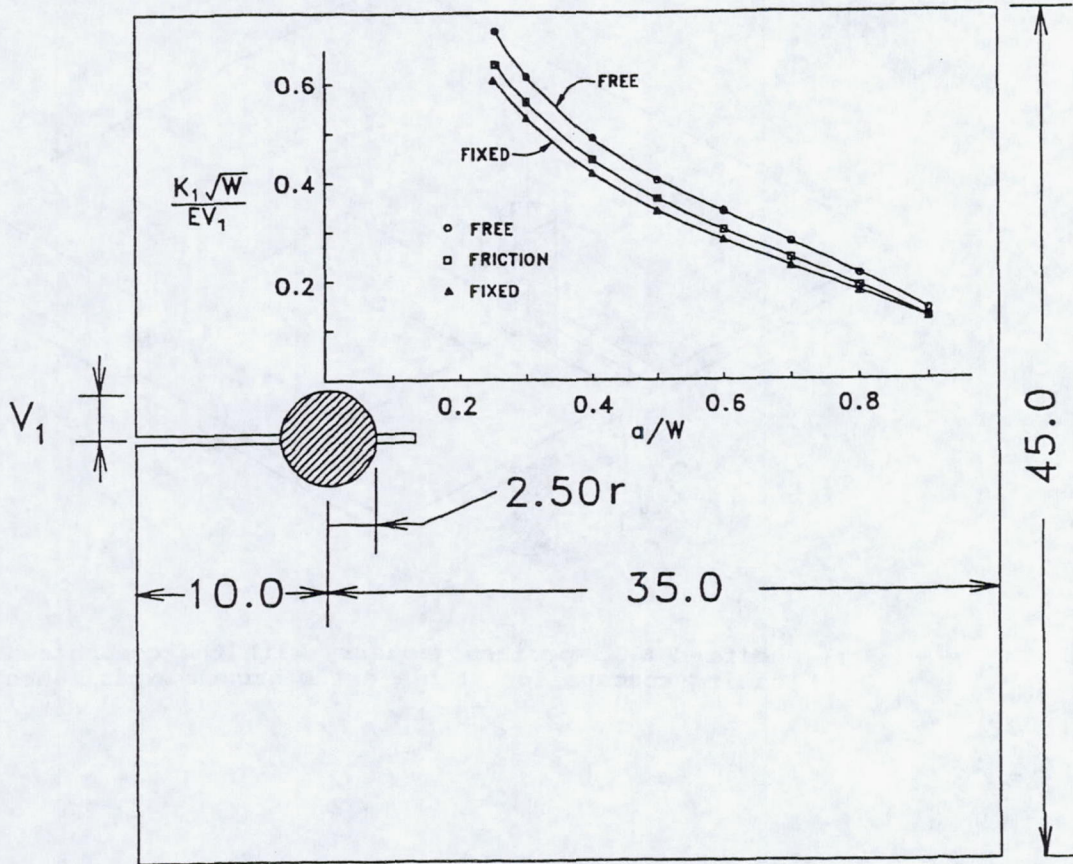


Fig. (3) Original SPL specimen geometry and numerical solution for normalized stress intensity factor as a function of normalized crack length.

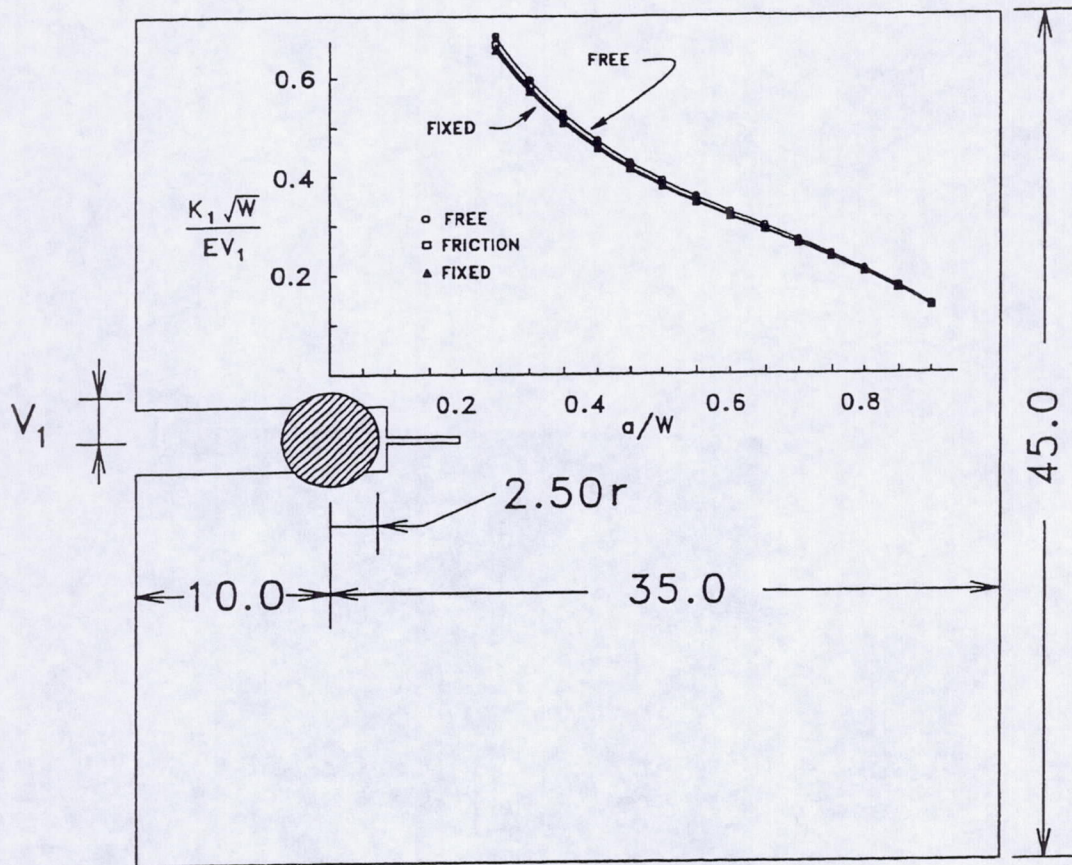


Fig. (4) Modified SPL specimen geometry and numerical solution for normalized stress intensity factor as a function of normalized crack length.

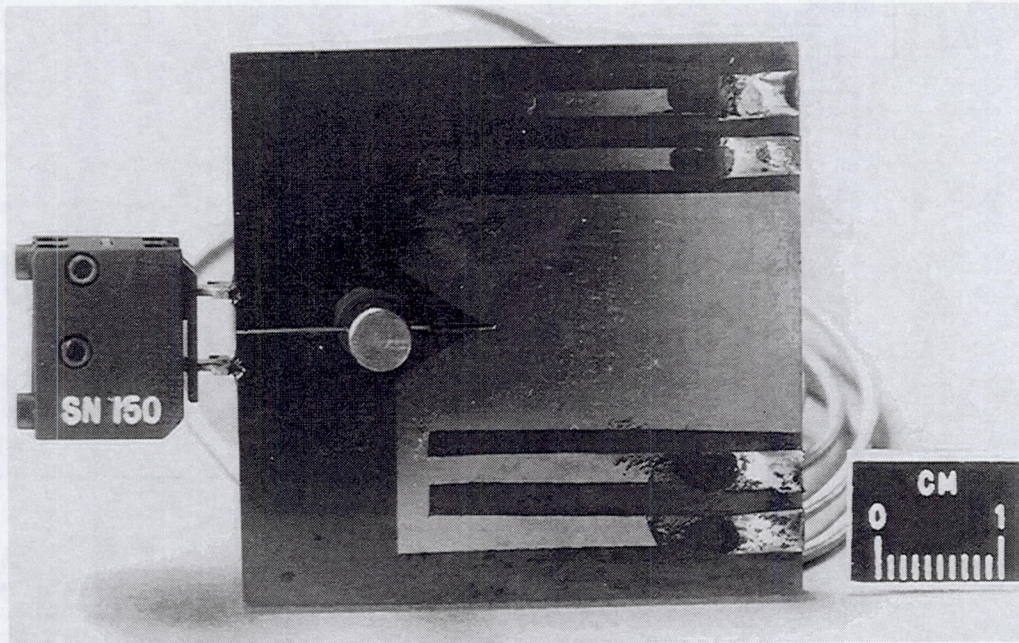


Fig (5) SPL specimen with commercial instrumentation for measuring crack mouth opening displacement.

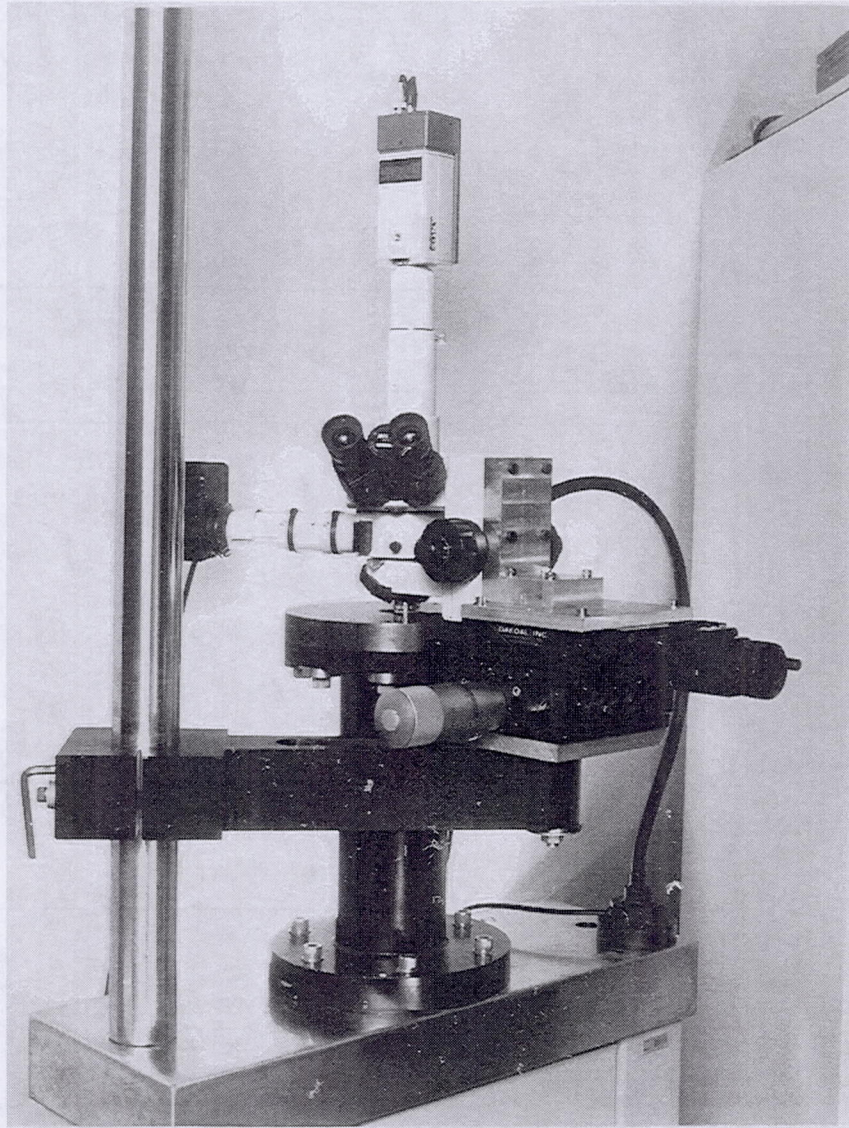


Fig (6) Test rig and traveling microscope used to conduct SPL fracture tests at room temperature.

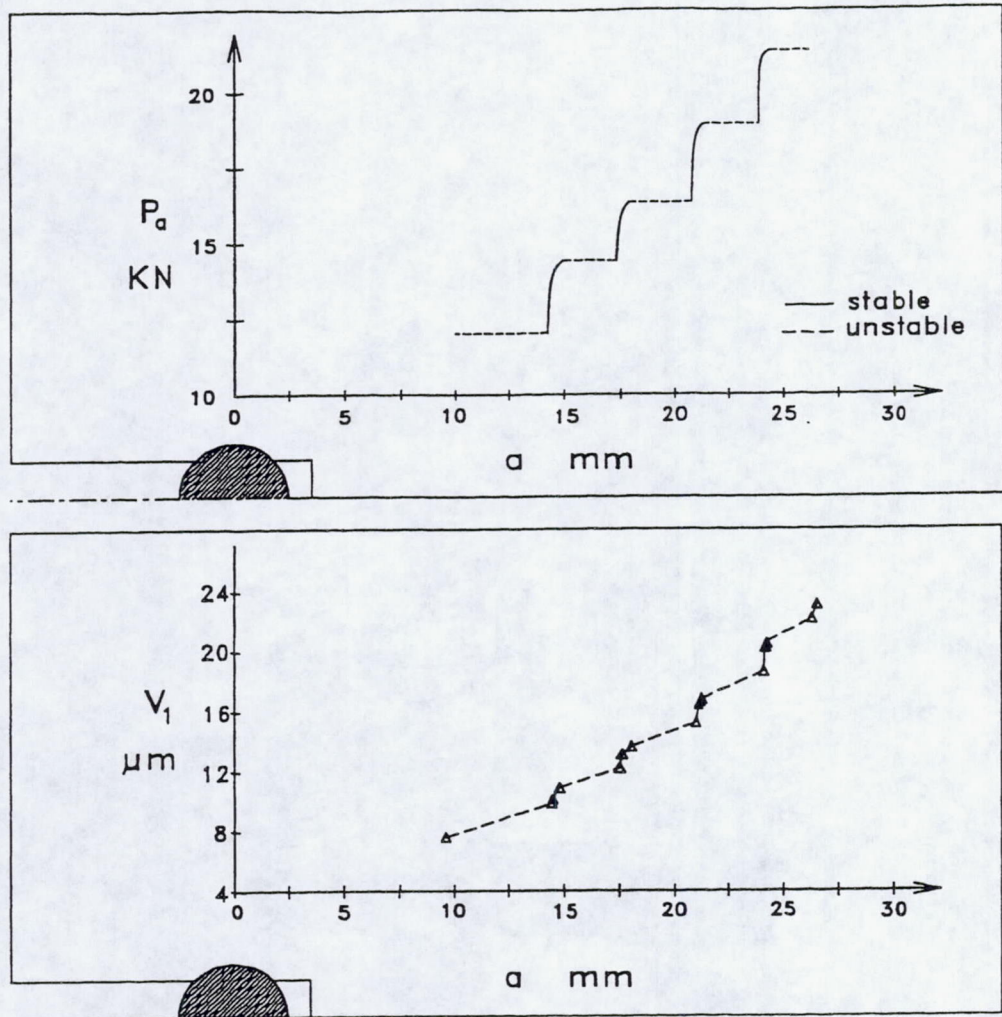


Fig. (7) Typical experimental results for crack mouth opening displacement versus load for the silicon nitride material. Specimen scale is provided for clarity of results.

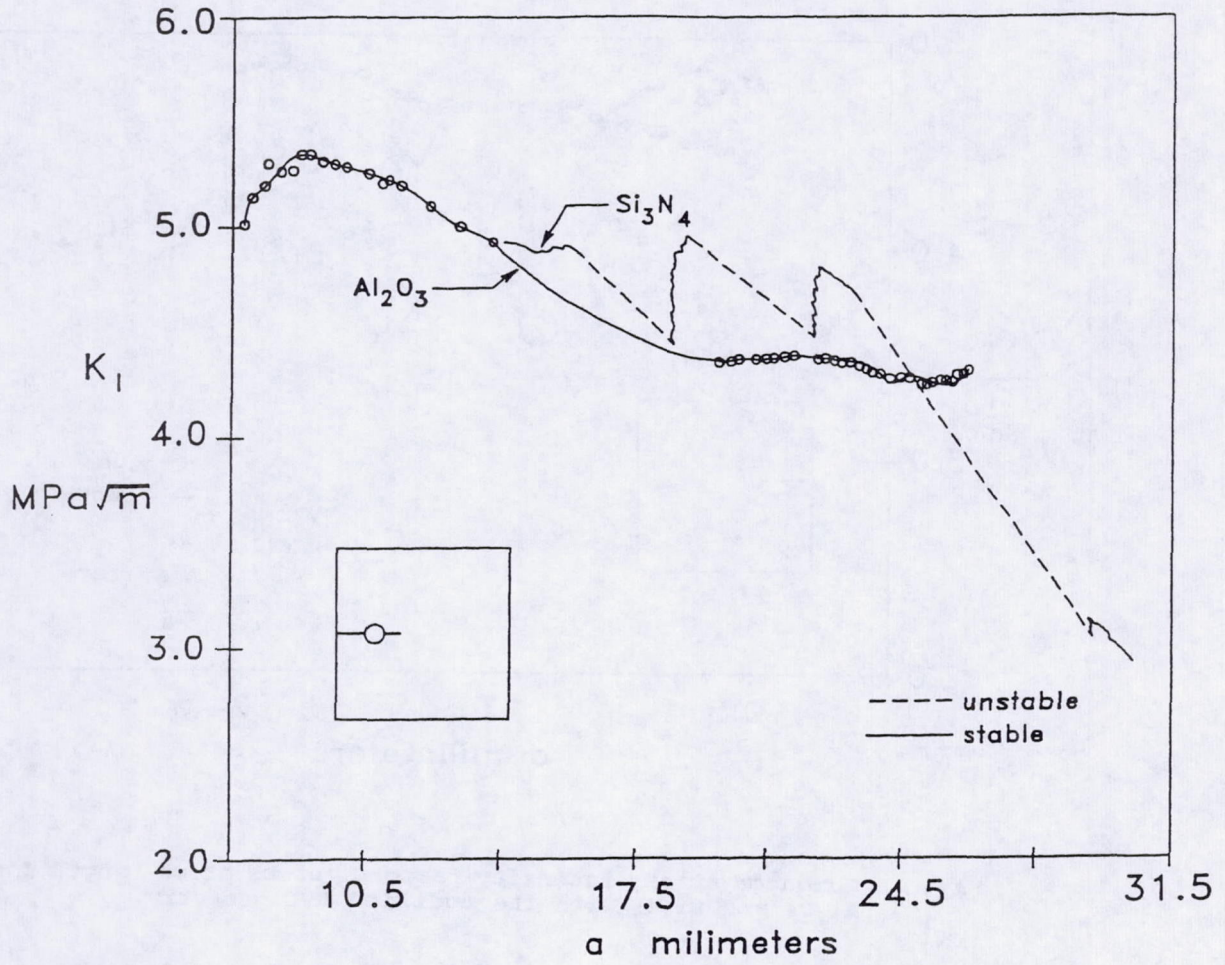


Fig. (8) Computed stress intensity factors versus crack length for Al_2O_3 and Si_3N_4 with the original SPL geometry.

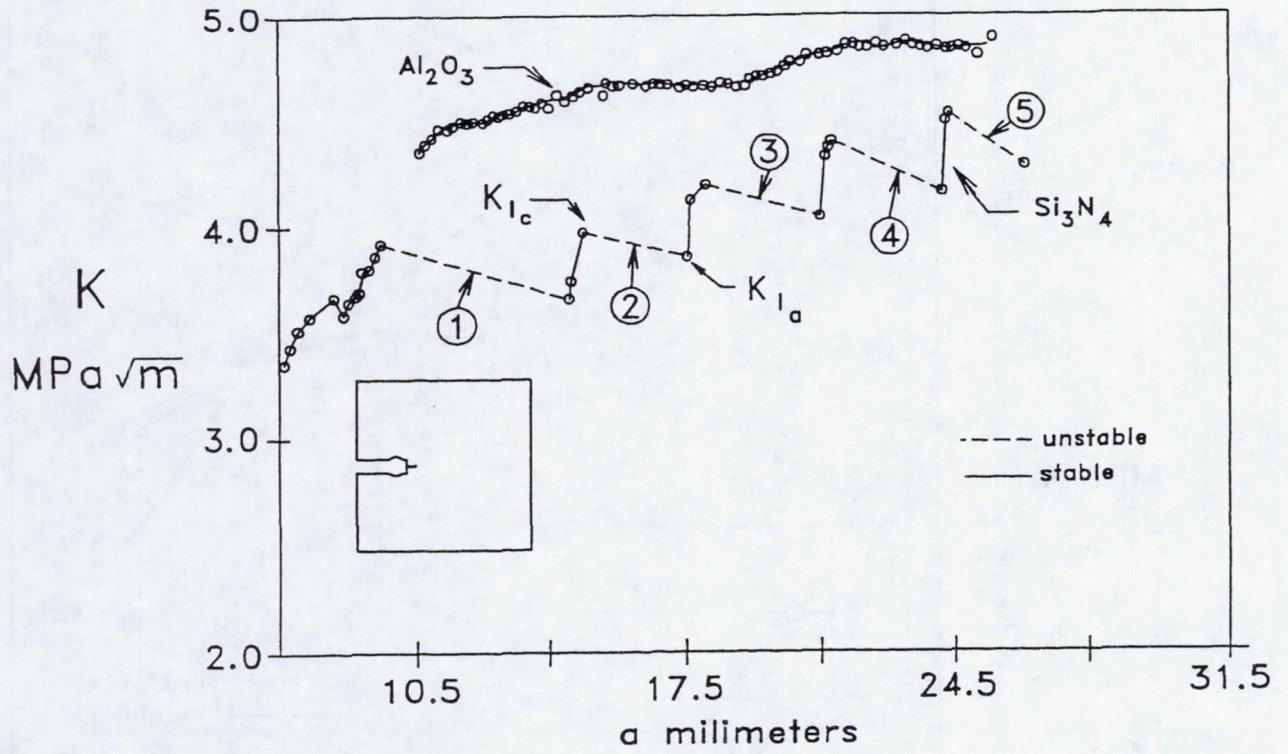


Fig. (9) Computed stress intensity factors versus crack length for Al_2O_3 and Si_3N_4 with the modified SPL geometry.

REPORT DOCUMENTATION PAGE

Form Approved
OMB No. 0704-0188

Public reporting burden for this collection of information is estimated to average 1 hour per response, including the time for reviewing instructions, searching existing data sources, gathering and maintaining the data needed, and completing and reviewing the collection of information. Send comments regarding this burden estimate or any other aspect of this collection of information, including suggestions for reducing this burden, to Washington Headquarters Services, Directorate for Information Operations and Reports, 1215 Jefferson Davis Highway, Suite 1204, Arlington, VA 22202-4302, and to the Office of Management and Budget, Paperwork Reduction Project (0704-0188), Washington, DC 20503.

1. AGENCY USE ONLY (Leave blank)	2. REPORT DATE July 1994	3. REPORT TYPE AND DATES COVERED Technical Memorandum	
4. TITLE AND SUBTITLE Fracture Behavior of Ceramics Under Displacement Controlled Loading		5. FUNDING NUMBERS WU-505-63-6B	
6. AUTHOR(S) Anthony Calomino, David Brewer and Louis Ghosn			
7. PERFORMING ORGANIZATION NAME(S) AND ADDRESS(ES) NASA Lewis Research Center Cleveland, Ohio 44135-3191 and Vehicle Propulsion Directorate U.S. Army Research Laboratory Cleveland, Ohio 44135-3191		8. PERFORMING ORGANIZATION REPORT NUMBER E-8976	
9. SPONSORING/MONITORING AGENCY NAME(S) AND ADDRESS(ES) National Aeronautics and Space Administration Washington, D.C. 20546-0001 and U.S. Army Research Laboratory Adelphi, Maryland 20783-1145		10. SPONSORING/MONITORING AGENCY REPORT NUMBER NASA TM-105565 ARL-MR-15	
11. SUPPLEMENTARY NOTES Anthony Calomino, NASA Lewis Research Center, Cleveland, Ohio; David Brewer, Vehicle Propulsion Directorate, U.S. Army Research Laboratory, NASA Lewis Research Center; and Louis Ghosn, Sverdrup Technology, Inc., Lewis Research Center Group, 2001 Aerospace Parkway, Brookpark, Ohio 44142. Responsible person, Anthony Calomino, organization code 5220, (216) 433-3311.			
12a. DISTRIBUTION/AVAILABILITY STATEMENT Unclassified - Unlimited Subject Category 27		12b. DISTRIBUTION CODE	
13. ABSTRACT (Maximum 200 words) A Mode I fracture specimen and loading method has been developed which permits the observation of stable crack extension in monolithic and in situ toughened ceramics. The developed technique was used to conduct room temperature tests on commercial grade alumina (Coors' AD-995) and silicon nitride (Norton NC-132). The results of these tests are reported. Crack growth for the alumina remained subcritical throughout testing revealing possible effects of environmental stress corrosion. The crack growth resistance curve for the alumina is presented. The silicon nitride tests displayed a series of stable (slow) crack growth segments interrupted by dynamic (rapid) crack extension. Crack initiation and arrest stress intensity factors, K_{Ic} and K_{Ia} , for silicon nitride are reported. The evolution of the specimen design through testing is briefly discussed.			
14. SUBJECT TERMS Controlled displacement; Fracture; Stable crack growth; Mode I		15. NUMBER OF PAGES 26	
		16. PRICE CODE A03	
17. SECURITY CLASSIFICATION OF REPORT Unclassified	18. SECURITY CLASSIFICATION OF THIS PAGE Unclassified	19. SECURITY CLASSIFICATION OF ABSTRACT Unclassified	20. LIMITATION OF ABSTRACT